● RESEARCH ARTICLE

Knocking down TRPM2 expression reduces cell injury and NLRP3 inflammasome activation in PC12 cells subjected to oxygen-glucose deprivation

Tao Pan[1, #], Qiu-Jiao Zhu[2, #], Li-Xiao Xu[3], Xin Ding[1], Jian-Qin Li[4], Bin Sun[1], Jun Hua[2, *], Xing Feng[1, *]

1 Department of Neonatology, Children's Hospital Affiliated to Suzhou University, Suzhou, Jiangsu Province, China
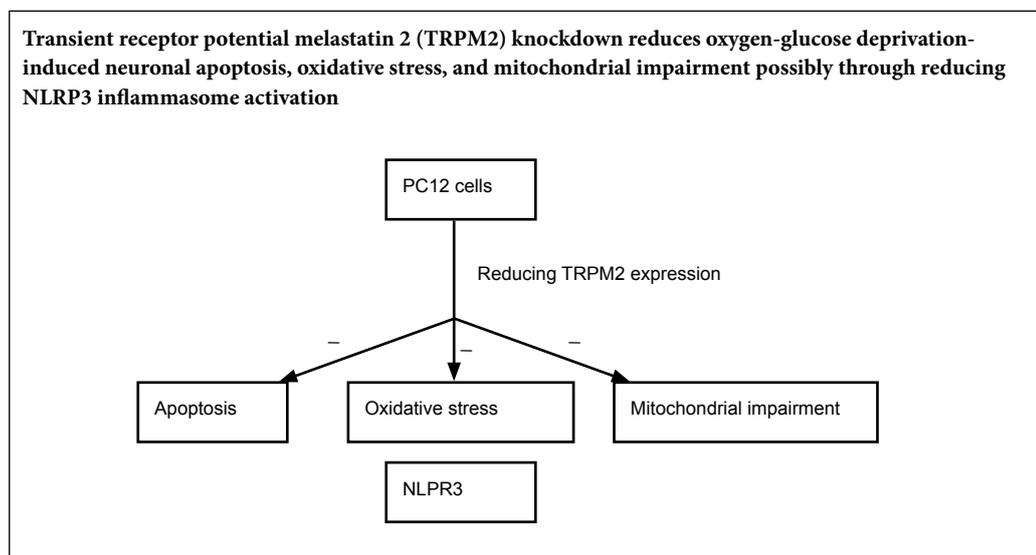2 Department of Critical Care Medicine, Children's Hospital Affiliated to Suzhou University, Suzhou, Jiangsu Province, China
3 Institute of Pediatrics, Children's Hospital Affiliated to Suzhou University, Suzhou, Jiangsu Province, China
4 Blood Section, Children's Hospital Affiliated to Suzhou University, Suzhou, Jiangsu Province, China

Graphical Abstract

Transient receptor potential melastatin 2 (TRPM2) knockdown reduces oxygen-glucose deprivation-induced neuronal apoptosis, oxidative stress, and mitochondrial impairment possibly through reducing NLRP3 inflammasome activation

Abstract

Transient receptor potential melastatin 2 (TRPM2) is an important ion channel that represents a potential target for treating injury caused by cerebral ischemia. However, it is unclear whether reducing TRPM2 expression can help repair cerebral injury, and if so what the mechanism underlying this process involves. This study investigated the protective effect of reducing TRPM2 expression on pheochromocytoma (PC12) cells injured by oxygen-glucose deprivation (OGD). PC12 cells were transfected with plasmid encoding TRPM2 shRNAS, then subjected to OGD by incubation in glucose-free medium under hypoxic conditions for 8 hours, after which the cells were allowed to reoxygenate for 24 hours. Apoptotic cells, mitochondrial membrane potentials, reactive oxygen species levels, and cellular calcium levels were detected using flow cytometry. The relative expression of C-X-C motif chemokine ligand 2 (CXCL2), NACHT, LRR, and PYD domain–containing protein 3 (NALP3), and caspase-1 were detected using fluorescence-based quantitative reverse transcription-polymerase chain reaction and western blotting. The rates of apoptosis, mitochondrial membrane potentials, reactive oxygen species levels, and cellular calcium levels in the TRPM2-shRNA + OGD group were lower than those observed in the OGD group. Taken together, these results suggest that TRPM2 knockdown reduces OGD-induced neuronal injury, potentially by inhibiting apoptosis and reducing oxidative stress levels, mitochondrial membrane potentials, intracellular calcium concentrations, and NLRP3 inflammasome activation.

Key Words: *apoptosis; calcium; caspase-1; NLRP3; mitochondrial impairment; oxidative stress; oxygen-glucose deprivation; PC12; shRNA; TRPM2*

Chinese Library Classification No. *R446; R363; R364*

Introduction

Cerebral ischemic injury is a sudden interruption of cerebral circulation caused by a variety of internal and external causes that result in insufficient or even absent blood supply (Kunz and Iadecola, 2009). Local blood and oxygen content decreased rapidly, which leads to cerebral ischemia and hypoxia (Zhao et al., 2017). Pathological changes caused by ischemic injury include calcium overloading, energy imbalance, release of glutamic acid, carbon monoxide poisoning, lipid peroxidation, oxygen free radical damage, and inflammation (Marin and Carmichael, 2018). When ischemia occurs, many neurons, especially those in the hippocampus and striatum, are damaged, which seriously affects the basic functions of the brain (Nguyen et al., 2018). As neurons do not have energy reserves, they tend to die when deprived of glucose and oxygen for a prolonged period.

Transient receptor potential melastatin (TRPM) ion channels constitute the largest transient receptor potential (TRP) subfamily, and are involved in many physiological processes (Kamm and Siemens, 2017). Transient receptor potential melastatin 2 (TRPM2), a member of the TRPM subfamily, is a non-selective cation channel that is extensively expressed on cell membranes (Aminzadeh et al., 2018). TRPM2 is an oxidative stress effector and can be activated by reactive oxygen species (ROS) (Xia et al., 2019). TRPM2 is the most abundant TRP channel in the brain and is sensitive to oxidative stress, which suggests that it could be an important therapeutic target for neurodegenerative diseases (Jiang et al., 2017; Mortadza et al., 2017; Belrose and Jackson, 2018). Intracellular calcium levels drive TRPM2 activity, which also depends on the presence of extracellular hydrogen peroxide (Wehage et al., 2002; McHugh et al., 2003). TRPM2 is responsible for the non-painful warmth sensitivity of somatosensory neurons (Tan and McNaughton, 2016). Additionally, TRPM2 is thought to act as a hypothalamic temperature sensor (Song et al., 2016). Other TRPM subfamily members, such as TRPM4, have been reported to play roles in ischemic stroke (Loh et al., 2014). However, the effects of directly reducing TRPM2 expression levels on cellular activity and downstream inflammatory reactions have not been fully investigated.

TRPM2 has been proposed as a treatment target for cerebral ischemic injury (Akpinar et al., 2016; Shimizu et al., 2016; Huang et al., 2017). However, it is unknown whether reducing TRPM2 expression could help repair cerebral injury, and if so what the mechanism underlying this process involves. In this study, hippocampal pheochromocytoma (PC12) cells were subjected to oxygen-glucose deprivation (OGD), and the effects of reducing TRPM2 expression on apoptosis, mitochondrial membrane potentials, ROS levels, cellular calcium levels, and inflammasome expression were investigated. The *in vitro* OGD model used in this study is useful for studying cerebral ischemic injury, as it is simple to grow, low-cost, and only requires a short experimental period. TRPM2 is expressed in neurons, as well as in glial cells, which regulate synaptic plasticity and cell survival in the hippocampus (Naziroglu et al., 2012). TRPM2 also participates in neuronal development and can inhibit neuronal growth. The physiological activation of microglia following exposure to ROS or treatment with LPS promotes nitric oxide production (Yamamoto et al., 2008; Haraguchi et al., 2012).

Materials and Methods

Cell lines

PC12 cells were purchased from Beina Biology (BNCC337644, Beina Biotech, Beijing, China) and cultured in RPMI1640 (KeyGENBioTECH, Nanjing, China) with 10% fetal bovine serum (Biological Industries, Beijing, China) in 5% CO_2 at 37°C, as previously described (Wang et al., 2011). Cells were grown to 60% confluence for used in experiments.

Construction of TRPM2 shRNAs

Three pairs of shRNA primers were designed based on the *TRPM2* gene sequence (**Table 1**). The sequences of PCR products were encoded in lentiviruses. PC12 cells were transfected with lentiviruses encoding the TRPM2-shRNAs using Lipofectamine®2000 (Invitrogen, Shanghai, China) for a final TRPM2-shRNA concentration of 1×10^6 IFU/PFU/mL. At 6 hours after transfection, the medium was replaced with fresh RPMI1640 containing 10% fetal bovine serum, and the cells were cultured for an additional 24 hours. TRPM2 expression was determined by quantitative reverse transcription-polymerase chain reaction (qRT-PCR) and western blotting.

Experimental groups

The cells were seeded into 24-well plates at a concentration of 3×10^5/mL. After the cells had completely adhered to the

Table 1 Sequences of TRPM2-shRNAs

Primers	Sequence (5′–3′)	Product size (bp)
sh-TRPM2-F1	GAT CCG CAC TCT GCA TAC CAT CTA CAC TTC CTG	65
	TCA GAT GTA GAT GGT ATG CAG AGT GCT TTT TG	
sh-TRPM2-R1	AAT TCA AAA AGC ACT CTG CAT ACC ATC TAC ATC	65
	TGA CAG GAA GTG TAG ATG GTA TGC AGA GTG CG	
sh-TRPM2-F2	GAT CCG CGG ATG AGT TTG AGC ATA GAC TTC CTG	65
	TCA GAT CTA TGC TCA AAC TCA TCC GCT TTT TG	
sh-TRPM2-R2	AAT TCA AAA AGC GGA TGA GTT TGA GCA TAG ATC	65
	TGA CAG GAA GTC TAT GCT CAA ACT CAT CCG CG	
sh-TRPM2-F3	GAT CCG TGT GTG AAG TTG CCT CAA TCC TTC CTG	65
	TCA GAG ATA TTC ATG TCA AGA CCA GCT TTT TG	
sh-TRPM2-R3	AAT TCA AAA AGG TCG TGA AGT TGC TCA ATC TGA	65
	CAG GAA GGA TTG AGG CAA CTT CAC GAC CG	

F: Forward; R: reverse; TRPM2: transient receptor potential melastatin 2.

wells, the growth medium for the OGD group was replaced with low-glucose medium, and the cells were incubated in a three-gas incubator (5% CO_2, 1% O_2 and 94% N_2) for 24 hours. The cells were divided into six groups (*n* = 6): the control group, the shRNA-NC group (vector control), the TRPM2-shRNA group, the OGD group, the shRNA-NC + OGD group, and the TRPM2-shRNA + OGD group. When the cells reached 60% confluence, they were transfected with 1 μL/mL TRPM2-shRNA or control shRNA (Shanghai GenePharma Co., Ltd., Shanghai, China) using Lipofectamine® 2000 (Shanghai Jima Industrial Co., Ltd., Shanghai, China). At 24 hours after transfection, the PC12 cells were subjected to OGD (incubation in glucose-free medium under hypoxic conditions for 8 hours, followed by reoxygenation for 24 hours), as previously described (Singh et al., 2009). The control group did not receive any treatment. The cells in the shRNA-NC group were transfected with the control shRNA. The cells in the shRNA-NC + OGD and TRPM2-shRNA + OGD groups were subjected to OGD.

Fluorescence-based qRT-PCR
RNA was extracted using a Trizol kit (CW0580S, CWBIO, China), and cDNA was synthesized using a reverse transcription kit (Dalian Baosheng, Dalian, China) according to the manufacturer's instructions. Using the cDNA as template, the expression of *C-X-C motif chemokine ligand 2* (*CXCL2*), *NACHT, LRR, and PYD domain–containing protein 3* (*NALP3*), and *caspase-1* was detected by fluorescence-based qRT-PCR, and normalized to β-actin expression (Livak and Schmittgen, 2001). The primers used for this experiment are listed in **Table 2**. The reaction mix included 9.5 μL RNase-free dH_2O, 2 μL primers, 1 μL cDNA, and 12.5 μL 2× qPCR mixture. The qRT-PCR program was as follows: 95 °C denaturation for 10 seconds, 58°C annealing for 30 seconds, and 72°C extension for 60 seconds for 40 cycles. The $2^{-\Delta\Delta Ct}$ method was used to quantify the relative expression of target genes (Livak and Schmittgen, 2001; Zhu et al., 2015).

Western blot assay
Total protein was isolated by adding proteolysis solution to

each group of cells and incubating at 4°C for 30 minutes. After centrifugation at 1000 r/min for 10 minutes, the supernatant was collected. Protein samples were heated at 100°C for 10 minutes, and the protein concentration was quantified using a BCA protein assay kit (Beyotime Institute of Biotechnology, Shanghai, China). For each group, 25 μg protein was subjected to sodium dodecyl sulfate-polyacrylamide gel electrophoresis (8%), and then transferred to a nitrocellulose membrane, as previously described (Song et al., 2019). The nitrocellulose membrane was blocked with 5% nonfat milk. The membrane was then incubated with primary antibodies at 4°C overnight: mouse anti-β-actin mAb (reference, 1:1000, TA-09; ZSbio, Beijing, China), rabbit anti-TRPM2 polyclonal antibody (ion channel, 1:1000, DF7533; Affinity, Cincinnati, OH, USA), rabbit anti-NLRP3 polyclonal antibody (NLRP3 inflammasome subunit, 1:1000, AF4620; Affinity, Cincinnati, OH, USA), rabbit anti-caspase-1 mAb (NLRP3 inflammasome subunit, 1:1000, #2225, CST; Abcam, Danvers, MA, USA), and CXCL2 (C-X-C motif chemokine ligand 2, 1:1000, ab9777; Abcam). After washing, the membrane was incubated with an anti-rabbit IgG horseradish peroxidase-conjugated secondary antibody (1:100; ab131368; Abcam) or an anti-mouse IgG horseradish peroxidase-conjugated secondary antibody (1:100; ab131368; Abcam) for 2 hours at room temperature. The protein expression levels were calculated using ImageJ software (v1.50d, NIH, Bethesda, MD, USA). The target protein expression was normalized to β-actin expression based on grayscale analysis. The TRPM2 antibody was used to verify gene knockdown and assess protein expression in the experimental samples; the other antibodies were only used to assess protein expression in the experimental samples.

Apoptosis assessment
At 24 hours after OGD injury, PC12 cells were collected by trypsin digestion (Gibco; Thermo Fisher Scientific, Waltham, MA, USA). The collected cells were incubated with Annexin V-fluorescein isothiocyanate and propidium iodide (Beyotime Institute of Biotechnology, Ningbo, China) for 30 minutes in the dark. The rate of apoptosis was then detected using a flow cytometer (BD Biosciences, Franklin Lakes, NJ, USA), within 1 hour of the incubation step. The number of Annexin V[+]/propidium iodide^{−} cells was calculated to determine the rate of apoptosis.

Measurement of mitochondrial membrane potential
At 24 hours after OGD injury, the PC12 cells were collected. The cells were treated with 5 μL 5,5′,6,6′-tetrachloro-1,1′,3,3′-tetraethylbenzimidazolylcarbocyanine iodide (JC-1; Beyotime Institute of Biotechnology, Ningbo, China) at 37°C for 15 minutes. JC-1 exhibits potential-dependent accumulation in mitochondria, indicated by a fluorescence emission shift from green (529 nm) to red (590 nm). Consequently, mitochondrial depolarization is indicated by a decrease in the red/green fluorescence intensity ratio. Mitochondrial membrane potential, as determined by the number of green cells, was detected within 1 hour of the incubation step.

Table 2 Sequences of the primers

Genes	Primer sequence (5′–3′)	Product size (bp)
CXCL2	Forward: ACA TCC AGA GCT TGA CGG TG	251
	Reverse: CAG GTA CGA TCC AGG CTT CC	
NLRP3	Forward: CTC TGC ATG CCG TAT CTG GT	84
	Reverse: ATG TCC TGA GCC ATG GAA GC	
Caspase-1	Forward: GAC CGA GTG GTT CCC TCA AG	108
	Reverse: GAC GTG TAC GAG TGG GTG TT	
TRPM2	Forward: GTT ACC TTC ACC ATT GAC CCA G	261
	Reverse: GGC TCT TTC CTC ATC CTT TCT	
β-Actin	Forward: GAC CCT GAA GTA CCC CAT TG	
	Reverse: GGT CAT CTT TTC ACG GTT GG	166

ROS measurement

At 24 hours after OGD injury, the PC12 cells were collected and treated with 10 μM dichloro-dihydro-fluorescein diacetate (DCFH-DA) at 37°C for 15 minutes (Beyotime Institute of Biotechnology, Ningbo, China). Cellular ROS was detected within 1 hour of treatment by flow cytometry according to the kit's instructions (DCFH-DA assay kit, Thermo Fisher Scientific). The fluorescence values (absorbance units) represented the ROS levels.

Cellular calcium level measurement

At 24 hours after OGD injury, the PC12 cells were collected. BBcellProbeTMF3 dye (Beyotime Institute of Biotechnology, Ningbo, China) was diluted 2000-fold in GIBCO® Hank's Balanced Salt Solution (Gibco; Thermo Fisher Scientific) to generate a working solution. The working solution was added to the cells, which were then incubated at 37°C for 20 minutes. Next, the cells were incubated with a 5-fold volume of Hank's Balanced Salt Solution containing 1% fetal bovine serum for an additional 40 minutes. Then, the cells were suspended in Hank's Balanced Salt Solution, incubated at 37°C for 10 minutes, and analyzed using flow cytometry. The fluorescence values (absorbance units) detected by flow cytometry represented the cellular calcium levels.

Statistical analysis

All data are presented as the mean ± SD. The differences among the six groups were determined by one-way analysis of variance followed by the Student-Newman-Keuls *post hoc* test using SPSS software, version 17.0 (SPSS, Inc., Chicago, IL, USA). $P < 0.05$ was considered statistically significant.

Results

TRPM2-shRNA-1 reduces TRPM2 expression in PC12 cells

TRPM2 mRNA expression in the TRPM2-shRNA-1 group was significantly lower than that in the control and shRNA-NC groups (**Figure 1**). TRPM2 protein expression in the OGD, shRNA-NC + OGD, and TRPM2-shRNA + OGD groups was lower than that in the shRNA-NC group ($P < 0.05$), and the effect was strongest when TRPM2-shRNA-1 was used (approximately 50% reduction in TRPM2 protein expression). Thus, TRPM2-shRNA-1 was selected for use in the following experiments.

TRPM2-shRNA-1 reduces OGD-induced apoptosis in PC12 cells

The rate of apoptosis was determined by flow cytometric analysis of annexin V and PI fluorescence. Compared with the control group (3.03%), the rate of apoptosis was significantly higher in the OGD (21.5%) and sh-NC + OGD groups (26.8%; **Figure 2**). Compared with the sh-NC + OGD group, the rate of apoptosis was significantly lower in the TRPM2-shRNA + OGD group (16.4%; $P < 0.05$).

TRPM2-shRNA-1 reduces OGD-induced impairment of mitochondrial membrane potential

Mitochondrial membrane potential was determined by flow cytometric analysis of JC-1 fluorescence. Compared with the control group (10.7%), the mitochondrial membrane potential (as determined by the number of green cells) was significantly higher in the OGD (40.7%) and sh-NC + OGD groups (39.2%; **Figure 3**). Compared with the sh-NC + OGD group, the mitochondrial membrane potential was significantly lower in the TRPM2-shRNA + OGD group (30.8%, $P < 0.05$).

TRPM2-shRNA-1 reduces OGD-induced ROS production

ROS levels were determined by flow cytometric analysis of DCFH-DA fluorescence. The ROS production in the OGD and sh-NC + OGD groups was higher than that in the control group (by approximately 5-fold; **Figure 4**). The ROS production in the TRPM2-shRNA + OGD group was lower than that in the sh-NC + OGD group (an approximately 24% decrease; $P < 0.05$).

TRPM2-shRNA-1 reduces OGD-induced cellular calcium levels

Cellular calcium levels were determined by flow cytometric analysis of BBcellProbeTMF3 fluorescence. Compared with the control group, cellular calcium levels were significantly higher in the OGD and sh-NC + OGD groups (an approximately 30% increase; **Figure 5**). Compared with the OGD group, cellular calcium levels were lower in the TRPM2-shRNA + OGD group than those in the sh-NC + OGD group (an approximately 19% reduction; $P < 0.05$). TRPM2-shRNA also reduced the basal calcium level compared with sh-NC (an approximately 40% reduction; $P < 0.05$).

TRPM2-shRNA-1 reduces OGD-induced expression of CXCL2, NLRP3, and caspase-1

Expression of CXCL2, NLRP3, and caspase-1 at both the mRNA and the protein level was evaluated. The expressions of CXCL2, NLRP3, and caspase-1 at the mRNA and the protein level were higher in the OGD and sh-NC + OGD groups than in the control group (**Figure 6**). The expressions of CXCL2, NLRP3, and caspase-1 at the mRNA and the protein level were significantly lower in the TRPM2-shRNA + OGD group than in the OGD group ($P < 0.05$). Compared with sh-NC, TRPM2-shRNA also significantly reduced CXCL2, NLRP3, and caspase-1 expression in cells that were not subjected to OGD ($P < 0.05$).

Discussion

The results from this study show that TRPM2 knockdown reduced OGD-induced neuronal injury, decreased the rate of apoptosis, reduced oxidative stress, and ameliorated mitochondrial impairment. We also showed that TRPM2 knockdown reduced OGD-induced expression of the NLRP3 inflammatory complex and CXCL2.

In the present study, the effect of TRPM2 knockdown on PC12 cells was investigated. TRPM2 knockdown was verified by fluorescence-based qRT-PCR and western blotting. TRPM2-shRNA-1 was selected for use in the majority of the experiments described here because it induced a greater level
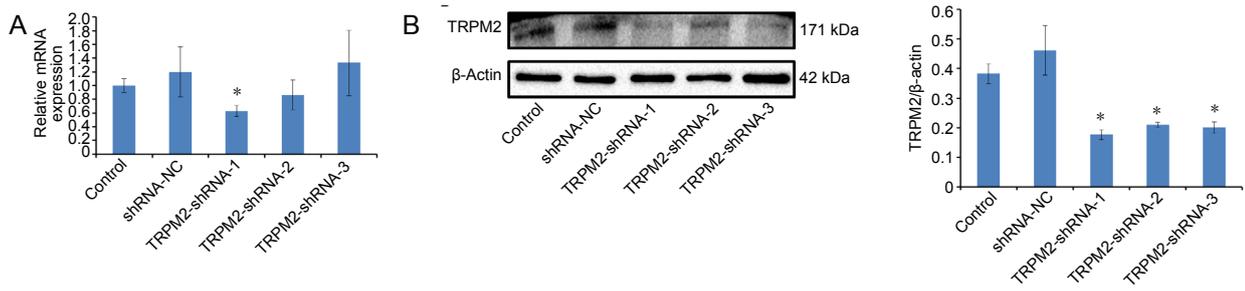
Figure 1 Verification of TRMP2 knockdown efficiency.
(A) TRPM2 mRNA expression (fluorescence-based quantitative reverse transplantation-polymerase chain reaction). (B) TRPM2 protein expression. TRPM2 expression was normalized to β-actin expression based on grayscale analysis. Data are expressed as the mean ± standard deviation (SD) (n = 6; one-way analysis of variance followed by Student-Newman-Keuls *post hoc* test). ∗$P < 0.05$, *vs.* shRNA-NC group. NC: Normal control; OGD: oxygen-glucose deprivation; PC12: pheochromocytoma; TRPM2: transient receptor potential melastatin 2.
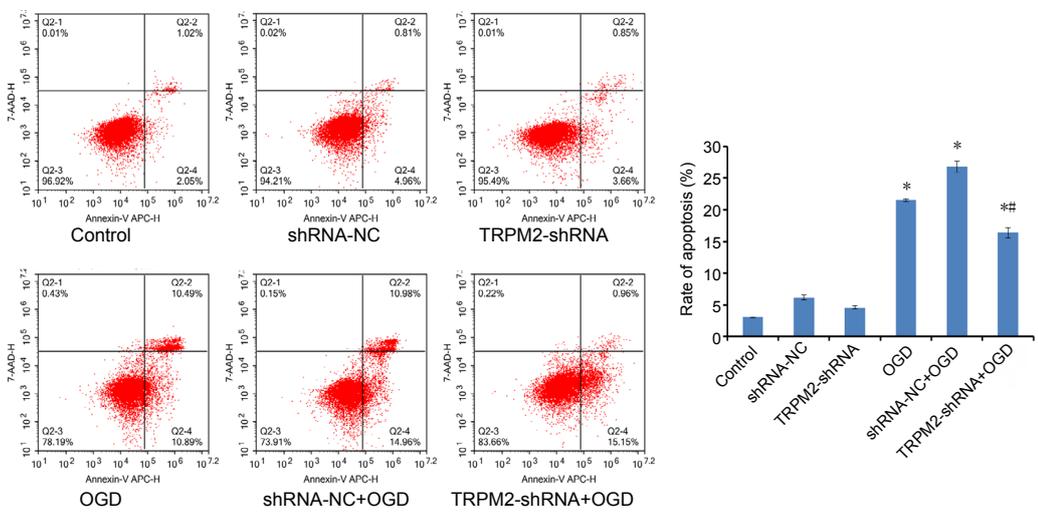
Figure 2 TRPM2-shRNA-1 reduces OGD-induced apoptosis in PC12 cells.
Representative flow cytometry images are shown on the left; Right: quantitative data. Data are expressed as the mean ± standard deviation (SD) (n = 6; one-way analysis of variance followed by Student-Newman-Keuls *post hoc* test). ∗$P < 0.05$, *vs.* shRNA-NC group; #$P < 0.05$, *vs.* shRNA-NC + OGD group. NC: Normal control; OGD: oxygen-glucose deprivation; PC12: pheochromocytoma; TRPM2: transient receptor potential melastatin 2.
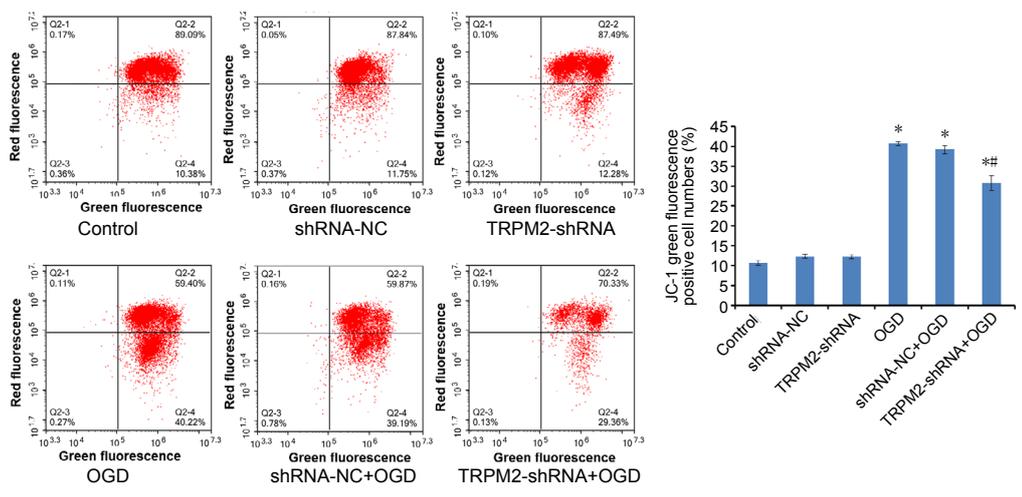
Figure 3 TRPM2-shRNA-1 reduces OGD-induced impairment of mitochondrial membrane potential.
(A) Representative flow cytometry images. (B) Quantitative data based on cells exhibiting JC-1 green florescence. Data are expressed as the mean ± standard deviation (SD) (n = 6; one-way analysis of variance followed by Student-Newman-Keuls *post hoc* test). ∗$P < 0.05$, *vs.* shRNA-NC group; #$P < 0.05$, *vs.* shRNA-NC + OGD group. NC: Normal control; OGD: oxygen-glucose deprivation; TRPM2: transient receptor potential melastatin 2.

of knockdown compared with the other two shRNAs tested.

Under normal physiological conditions, ROS is produced at low levels and regulates signal transduction and metabolism, as well as neuronal synaptic transmission (Cadenas, 2018). However, during ischemia and in the post-ischemia reperfusion phase, large amounts of ROS are produced, which can directly attack intracellular proteins and liposomes and indirectly modulate intracellular signaling

pathways (Pisarenko et al., 2015). The mitochondria are important sources of ROS during ischemia and reperfusion. Intracellular calcium overloading and other stimuli can impair mitochondrial function and results in the production of large amounts of ROS (Cao et al., 2011). Mitochondrial ROS also elicit mitochondrial cytochrome c release, thereby promoting apoptosis (Zhu et al., 2010).

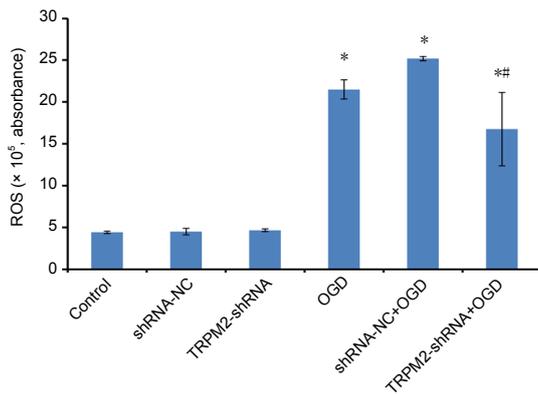Neuronal damage, as recapitulated in the OGD model,

Figure 4 TRPM2-shRNA-1 reduces OGD-induced ROS production.
Data are expressed as the mean ± standard deviation (SD) (n = 6; one-way analysis of variance followed by Student-Newman-Keuls *post hoc* test). ∗P < 0.05, *vs.* shRNA-NC group; #P < 0.05, *vs.* shRNA-NC + OGD group. NC: Normal control; OGD: oxygen-glucose deprivation; ROS: reactive oxygen species; TRPM2: transient receptor potential melastatin 2.
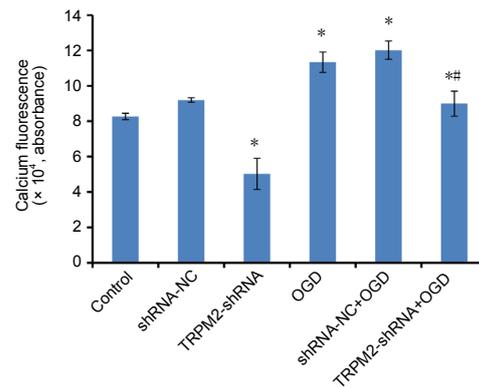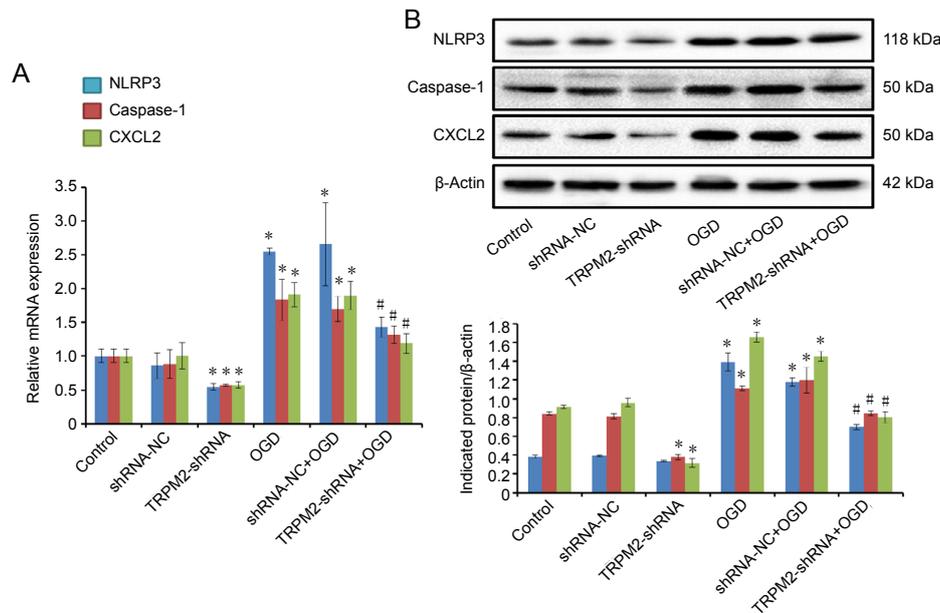

Figure 5 TRPM2-shRNA-1 reduces OGD-induced cellular calcium level.
Data are expressed as the mean ± standard deviation (SD) (n = 6; one-way analysis of variance followed by Student-Newman-Keuls *post hoc* test). ∗P < 0.05, *vs.* shRNA-NC group; #P < 0.05, *vs.* shRNA-NC + OGD group. NC: Normal control; OGD: oxygen-glucose deprivation; TRPM2: transient receptor potential melastatin 2.

Figure 6 TRPM2-shRNA-1 reduces OGD-induced expression of NLRP3, CXCL2, and caspase-1.
(A) NLRP3 (NLRP3/β-actin), CXCL2 (CXCL2/β-actin), and caspase-1 (caspase-1/β-actin) mRNA expression (as determined by fluorescence-based quantitative reverse transcription-polymerase chain reaction). (B) NLRP3, CXCL2, and caspase-1 protein expression (as determined by western blotting). Data are expressed as the mean ± standard deviation (SD) (n = 6; one-way analysis of variance followed by Student-Newman-Keuls *post hoc* test). ∗P < 0.05, *vs.* shRNA-NC group; #P < 0.05, *vs.* shRNA-NC + OGD group. CXCL2: chemokine ligand-2; NC: normal control; NLRP3: NACHT, LRR and PYD domains-containing protein 3; OGD: oxygen-glucose deprivation; TRPM2: transient receptor potential melastatin 2.

can activate calcium activity, which leads to the activation of membrane receptors (Tanaka et al., 2009). ROS activates TRPM2 channels, which mediate oxidative stress-induced membrane depolarization, increasing cell membrane conductance and cellular calcium levels (Verma et al., 2012). Miller et al. (2014) showed that cardiac cell death is associated with TRPM2 activation. TRPM2 may also represent a link between calcium- and ROS-dependent signaling pathways (Hara et al., 2002). TRPM2 inhibition reduces infarct volume and neuronal apoptosis (Luo et al., 2018). Jia et al. (2011) found that TRPM2 inhibition can reduce damage to CA1 neurons in the hippocampus of male mice, which suggests that TRPM2 inhibitors could be used as neuroprotective agents to protect against ischemic injury. In our study we found that OGD increased the rate of apoptosis, mitochondrial membrane potentials, cellular ROS levels,

and calcium levels, and that these effects were mitigated by TRPM2 knockdown. These results suggest that OGD can promote ROS production, activate calcium signaling, and induce apoptosis in PC12 cells. Inhibiting TRPM2 expression decreased calcium channel activation and reduced ROS production, ultimately protecting PC12 cells from apoptosis.

NLRP3 is a member of the NOD-like family of intracytoplasmic pattern recognition receptors. Upon activation NLRP3, inactive caspase-1 is recruited by adaptor protein apoptosis–associated speck-like protein to form the NLRP3 inflammatory complex. This complex induces cleavage of the precursor of caspase-1, generating the active molecule. In this study, we assessed total caspase-1 levels to determine the level of NLRP3 inflammasome activity. Caspase-1 can cleave the interleukin-18 and interleukin-1β precursors into their active forms, which are then incorporated into the classical

NLRP3 inflammatory complex (Wen et al., 2011). NLRP3 expression increases during the onset of myocardial infarction, and the inflammatory complex is involved in the development of infarction injury (Tschopp and Schroder, 2010). The NLRP3 inflammatory complex also plays important roles in hepatic ischemic injury (Kim et al., 2014).

CXCL2 is an inflammatory chemokine, and its corresponding receptor CXC chemokine receptor 2 (CXCR2) is mainly expressed on the surface of inflammatory cells (Deftu et al., 2017). CXCL2 binding to the CXCR2 receptor promotes inflammation and aggravates cerebral ischemia. CXCL2 and CXCR2 expression increase after cerebral ischemia. CXCL2 binding to CXCR2 enhances its expression, and induces neutrophils, natural killer cells, dendritic cells, and other inflammatory cells to migrate to and aggregate at sites of ischemic injury (Boro and Balaji, 2017). Therefore, the inflammatory response is aggravated in injured areas (Boro and Balaji, 2017). When TRPM2 expression is down-regulated, CXCL2 expression is significantly reduced, which suggests that TRPM2 regulates CXCL2 expression (Gershkovitz et al., 2019). TRPM2 is required for ROS-induced CXCL2 expression in monocytes (Knowles et al., 2013). Here we showed that NLRP3, caspase-1, and CXCL2 increased expression increased when cells were subjected to OGD, and that these effects were mitigated by TRPM2 knockdown. These results suggest that OGD activates the NLRP3 inflammatory complex and increases CXCL2 expression. Interestingly, TRPM2 knockdown also appeared to affect cellular calcium levels and the expression of CXCL2, NLRP3, and caspase-1, but not apoptosis or ROS levels in cells that were not subjected to OGD. These results suggest that TRPM2 knockdown reduces calcium level and inhibits NLRP3 activity under both physiological and pathological conditions. TRPM2 knockdown did not affect basal levels of apoptosis, ROS production, and mitochondrial membrane polarization; however, the low levels of these processes under physiological conditions may have masked the effects of TRPM2 knockdown.

There were some limitations to this study. First, the exact mechanisms underlying the effects observed here were not investigated in detail. Although TRPM2 knockdown reduced the effects of OGD-induced neuronal injury, including increased apoptosis, oxidative stress, and mitochondrial impairment, it had less of an effect on NLRP3 inflammatory complex activity and CXCL2 expression. Second, the effects of TRPM2 knockdown were not assessed *in vivo*; an animal model of ischemic stroke should be used to explore this in the future.

In conclusion, TRPM2 knockdown reduces OGD-induced neuronal apoptosis, oxidative stress, and mitochondrial impairment, possibly by reducing NLRP3 inflammasome activation.

Author contributions: *Experimental implementation and data analysis: TP, QJZ, LXX, XD, JQL and BS; study design and manuscript writing: JH*

References

Akpinar H, Naziroglu M, Ovey IS, Cig B, Akpinar O (2016) The neuroprotective action of dexmedetomidine on apoptosis, calcium entry and oxidative stress in cerebral ischemia-induced rats: Contribution of TRPM2 and TRPV1 channels. Sci Rep 6:37196.

Aminzadeh M, Roghani M, Sarfallah A, Riazi GH (2018) TRPM2 dependence of ROS-induced NLRP3 activation in Alzheimer's disease. Int Immunopharmacol 54:78-85.

Belrose JC, Jackson MF (2018) TRPM2: a candidate therapeutic target for treating neurological diseases. Acta Pharmacol Sin 39:722-732.

Boro M, Balaji KN (2017) CXCL1 and CXCL2 regulate NLRP3 inflammasome activation via G-protein-coupled receptor CXCR2. J Immunol 199:1660-1671.

Cadenas S (2018) ROS and redox signaling in myocardial ischemia-reperfusion injury and cardioprotection. Free Radic Biol Med 117:76-89.

Cao XH, Zhao SS, Liu DY, Wang Z, Niu LL, Hou LH, Wang CL (2011) ROS-Ca(2+) is associated with mitochondria permeability transition pore involved in surfactin-induced MCF-7 cells apoptosis. Chem Biol Interact 190:16-27.

Deftu AF, Filippi A, Shibasaki K, Gheorghe RO, Chiritoiu M, Ristoiu V (2017) Chemokine (C-X-C motif) ligand 1 (CXCL1) and chemokine (C-X-C motif) ligand 2 (CXCL2) modulate the activity of TRPV1+/IB4+ cultured rat dorsal root ganglia neurons upon short-term and acute application. J Physiol Pharmacol 68:385-395.

Gershkovitz M, Fainsod-Levi T, Zelter T, Sionov RV, Granot Z (2019) TRPM2 modulates neutrophil attraction to murine tumor cells by regulating CXCL2 expression. Cancer Immunol Immunother 68:33-43.

Hara Y, Wakamori M, Ishii M, Maeno E, Nishida M, Yoshida T, Yamada H, Shimizu S, Mori E, Kudoh J, Shimizu N, Kurose H, Okada Y, Imoto K, Mori Y (2002) LTRPC2 Ca2+-permeable channel activated by changes in redox status confers susceptibility to cell death. Mol Cell 9:163-173.

Haraguchi K, Kawamoto A, Isami K, Maeda S, Kusano A, Asakura K, Shirakawa H, Mori Y, Nakagawa T, Kaneko S (2012) TRPM2 contributes to inflammatory and neuropathic pain through the aggravation of pronociceptive inflammatory responses in mice. J Neurosci 32:3931-3941.

Huang S, Turlova E, Li F, Bao MH, Szeto V, Wong R, Abussaud A, Wang H, Zhu S, Gao X, Mori Y, Feng ZP, Sun HS (2017) Transient receptor potential melastatin 2 channels (TRPM2) mediate neonatal hypoxic-ischemic brain injury in mice. Exp Neurol 296:32-40.

Jia J, Verma S, Nakayama S, Quillinan N, Grafe MR, Hurn PD, Herson PS (2011) Sex differences in neuroprotection provided by inhibition of TRPM2 channels following experimental stroke. J Cereb Blood Flow Metab 31:2160-2168.

Jiang Q, Gao Y, Wang C, Tao R, Wu Y, Zhan K, Liao M, Lu N, Lu Y, Wilcox CS, Luo J, Jiang LH, Yang W, Han F (2017) Nitration of TRPM2 as a molecular switch induces autophagy during brain pericyte injury. Antioxid Redox Signal 27:1297-1316.

Kamm GB, Siemens J (2017) The TRPM2 channel in temperature detection and thermoregulation. Temperature (Austin) 4:21-23.

Kim SR, Kim DI, Kim SH, Lee H, Lee KS, Cho SH, Lee YC (2014) NLRP3 inflammasome activation by mitochondrial ROS in bronchial epithelial cells is required for allergic inflammation. Cell Death Dis 5:e1498.

Knowles H, Li Y, Perraud AL (2013) The TRPM2 ion channel, an oxidative stress and metabolic sensor regulating innate immunity and inflammation. Immunol Res 55:241-248.

Kunz A, Iadecola C (2009) Cerebral vascular dysregulation in the ischemic brain. Handb Clin Neurol 92:283-305.

Livak KJ, Schmittgen TD (2001) Analysis of relative gene expression data using real-time quantitative PCR and the 2(-Delta Delta C(T)) Method. Methods 25:402-408.

Loh KP, Ng G, Yu CY, Fhu CK, Yu D, Vennekens R, Nilius B, Soong TW, Liao P (2014) TRPM4 inhibition promotes angiogenesis after ischemic stroke. Pflugers Arch 466:563-576.

Luo X, Li M, Zhan K, Yang W, Zhang L, Wang K, Yu P, Zhang L (2018) Selective inhibition of TRPM2 channel by two novel synthesized ADPR analogues. Chem Biol Drug Des 91:552-566.

Marin MA, Carmichael ST (2018) Stroke in CNS white matter: Models and mechanisms. Neurosci Lett 684:193-199.

McHugh D, Flemming R, Xu SZ, Perraud AL, Beech DJ (2003) Critical intracellular Ca2+ dependence of transient receptor potential melastatin 2 (TRPM2) cation channel activation. J Biol Chem 278:11002-11006.

Miller BA, Hoffman NE, Merali S, Zhang XQ, Wang J, Rajan S, Shanmughapriya S, Gao E, Barrero CA, Mallilankaraman K, Song J, Gu T, Hirschler-Laszkiewicz I, Koch WJ, Feldman AM, Madesh M, Cheung JY (2014) TRPM2 channels protect against cardiac ischemia-reperfusion injury: role of mitochondria. J Biol Chem 289:7615-7629.

Mortadza SS, Sim JA, Stacey M, Jiang LH (2017) Signalling mechanisms mediating Zn(2+)-induced TRPM2 channel activation and cell death in microglial cells. Sci Rep 7:45032.

Naziroglu M, Celik O, Ozgul C, Cig B, Dogan S, Bal R, Gumral N, Rodriguez AB, Pariente JA (2012) Melatonin modulates wireless (2.45 GHz)-induced oxidative injury through TRPM2 and voltage gated Ca(2+) channels in brain and dorsal root ganglion in rat. Physiol Behav 105:683-692.

Nguyen H, Zarriello S, Rajani M, Tuazon J, Napoli E, Borlongan CV (2018) Understanding the role of dysfunctional and healthy mitochondria in stroke pathology and its treatment. Int J Mol Sci 19:E2127.

Pisarenko O, Shulzhenko V, Studneva I, Pelogeykina Y, Timoshin A, Anesia R, Valet P, Parini A, Kunduzova O (2015) Structural apelin analogues: mitochondrial ROS inhibition and cardiometabolic protection in myocardial ischaemia reperfusion injury. Br J Pharmacol 172:2933-2945.

Shimizu T, Dietz RM, Cruz-Torres I, Strnad F, Garske AK, Moreno M, Venna VR, Quillinan N, Herson PS (2016) Extended therapeutic window of a novel peptide inhibitor of TRPM2 channels following focal cerebral ischemia. Exp Neurol 283:151-156.

Song K, Wang H, Kamm GB, Pohle J, Reis FC, Heppenstall P, Wende H, Siemens J (2016) The TRPM2 channel is a hypothalamic heat sensor that limits fever and can drive hypothermia. Science 353:1393-1398.

Song ZJ, Yang SJ, Han L, Wang B, Zhu G (2019) Postnatal calpeptin treatment causes hippocampal neurodevelopmental defects in neonatal rats. Neural Regen Res 14:834-840.

Tan CH, McNaughton PA (2016) The TRPM2 ion channel is required for sensitivity to warmth. Nature 536:460-463.

Tanaka K, Iijima T, Mishima T, Suga K, Akagawa K, Iwao Y (2009) Ca(2+) buffering capacity of mitochondria after oxygen-glucose deprivation in hippocampal neurons. Neurochem Res 34:221-226.

Tschopp J, Schroder K (2010) NLRP3 inflammasome activation: The convergence of multiple signalling pathways on ROS production? Nat Rev Immunol 10:210-215.

Verma S, Quillinan N, Yang YF, Nakayama S, Cheng J, Kelley MH, Herson PS (2012) TRPM2 channel activation following in vitro ischemia contributes to male hippocampal cell death. Neurosci Lett 530:41-46.

Wang X, Zhu G, Yang S, Wang X, Cheng H, Wang F, Li X, Li Q (2011) Paeonol prevents excitotoxicity in rat pheochromocytoma PC12 cells via downregulation of ERK activation and inhibition of apoptosis. Planta Med 77:1695-1701.

Wehage E, Eisfeld J, Heiner I, Jungling E, Zitt C, Luckhoff A (2002) Activation of the cation channel long transient receptor potential channel 2 (LTRPC2) by hydrogen peroxide. A splice variant reveals a mode of activation independent of ADP-ribose. J Biol Chem 277:23150-23156.

Wen H, Gris D, Lei Y, Jha S, Zhang L, Huang MT, Brickey WJ, Ting JP (2011) Fatty acid-induced NLRP3-ASC inflammasome activation interferes with insulin signaling. Nat Immunol 12:408-415.

Xia S, Wang L, Fu TM, Wu H (2019) Mechanism of TRPM2 channel gating revealed by cryo-EM. FEBS J 286:3333-3339.

Yamamoto S, Shimizu S, Kiyonaka S, Takahashi N, Wajima T, Hara Y, Negoro T, Hiroi T, Kiuchi Y, Okada T, Kaneko S, Lange I, Fleig A, Penner R, Nishi M, Takeshima H, Mori Y (2008) TRPM2-mediated Ca2+ influx induces chemokine production in monocytes that aggravates inflammatory neutrophil infiltration. Nat Med 14:738-747.

Zhao GC, Yuan YL, Chai FR, Ji FJ (2017) Effect of Melilotus officinalis extract on the apoptosis of brain tissues by altering cerebral thrombosis and inflammatory mediators in acute cerebral ischemia. Biomed Pharmacother 89:1346-1352.

Zhu G, Wang X, Chen Y, Yang S, Cheng H, Wang N, Li Q (2010) Puerarin protects dopaminergic neurons against 6-hydroxydopamine neurotoxicity via inhibiting apoptosis and upregulating glial cell line-derived neurotrophic factor in a rat model of Parkinson's disease. Planta Med 76:1820-1826.